Cathodic Modifications of Platinum Surfaces in Organic Solvent: Reversibility and Cation Type Effects

J. Ghilane,[†] M. Guilloux-Viry,[‡] C. Lagrost,[†] P. Hapiot,*[,†] and J. Simonet[†]

Laboratoire d'Electrochimie Moléculaire et Macromoléculaire, Synthèse et Electrosynthèse Organiques, Unite Mixte de Recherche Centre National de la Recherche Scientifique−Université de Rennes 1 6510, Institut de Chimie de Rennes, Laboratoire de Chimie du Solide et Inorganique Moléculaire, Unite Mixte de Recherche Centre National de la Recherche Scientifique−Université de Rennes 1 6511, and Institut de Chimie de Rennes, Campus de Beaulieu, 35042 Rennes, France

Received: April 9, 2005; In Final Form: June 15, 2005

Cathodic modification of platinum surfaces leads to the formation of iono−platinic phases ([Pt_n^-, M^+, MX]), which involves the insertion of cations and salts into the platinum electrode. This process was investigated at the local scale by in situ observation of surface electrochemical processes by atomic force microscopy (EC-AFM) techniques as a function of the salt and the injected charge, with special attention about the process reversibility. AFM images recorded in solution after the cathodic modifications of well-defined platinum surfaces [epitaxial platinum deposit on (100) MgO substrate] show drastic modification on the morphology of the surface, confirming previous ex situ studies. The amplitude of the modifications directly depends on both the nature of supporting electrolyte and the quantity of charge injected into the platinum. As long as the injected charge remains small enough to maintain the adhesion of the Pt deposit onto the MgO substrate, the process was found to be fully reversible. Indeed, impressive morphology changes occur under the cathodic treatment (formation of [Pt_n^-, M^+, MX]) but the initial geometry is totally recovered after reoxidation of the iono−platinic phase. This cycle of reduction−reoxidation can be performed several times without any significant alteration of the recovered surface and of its structural characteristics. It is suggested that the modification starts at the interface solution platinum surface and then its insertion into the platinum surface.

Introduction

It has recently been shown that iono−metallic interfaces can be obtained by electrochemical treatment of noble metals, like platinum, in nonaqueous solvents containing organic or inorganic background electrolytes.[1] Even if the formation of such solid phases upon the cathodic reduction of metals is a common phenomenon (see for example the discovery of alkaline metals combination with posttransition metals made by Zintl at the beginning of the 20th century[2] or the results reported for other metallic materials[3]), this observation was unexpected for a metal that was commonly used as a noncorrodible cathodic material for decades.[4] The elemental electrochemical process, which formally corresponds to the reduction of the platinum metal, involves an electron transfer coupled with the insertion of the cation electrolyte M^+ and leads to the formation of iono−metallic phases of the general formula [Pt_n^-, M^+, MX] (where X^- is the anion of the supporting electrolyte).[1] This process occurs when the platinum electrode is held at negative potential in the presence of organic solvents under superdry conditions:

$$n\mathrm{Pt} + e^- + M^+ + MX \rightarrow [Pt_n^-, M^+, MX]$$

Platinum surface modifications were reported with several supporting electrolytes in dimethylformamide (DMF) and were investigated by different methods.[1] Techniques involving coulometry, electrochemical quartz crystal microbalance (EQCM), and electrochemical impedance spectroscopy[5] confirm the formation of the reduced platinum phases. The electrochemical process was followed through the simultaneous recordings of the charge−discharge currents and mass variations (combined use of classical electrochemical methods such as cyclic voltammetry and chronocoulometry and EQCM), which allowed the determination of the stoichiometry of the platinic compound.[1,6] The value of *n* in [Pt_n^-, M^+, MX] was found to be dependent on the electrolysis conditions and on the nature of the electrolyte. With thin layers of platinum deposited onto an inactive substrate, *n* was calculated to be close to 2. Scanning electron microscopy (SEM) was extensively used to observe the morphology of the platinum surfaces after the electrochemical treatment. The images evidenced impressive modifications of the metal surfaces.[1] However, this technique allows only the ex situ observation of the sample because the modified platinum electrode must be taken out of the solution, washed, and transferred from the electrochemical system to the microscope before the imaging. Besides the fact that some fine details may be lost in the sample preparation, there are other difficulties due to possible contaminations and the occurrence of secondary reactions of the organic−metal interface with atmospheric components (O_2, H_2O, CO_2, oxidation under air).[1b,d] It results that the modified materials continue to evolve as soon as the potential is not maintained at a negative value.[1] In addition, because the modified platinum surfaces are covered with iono−metallic phases that are electrically isolating, electronic charging of the sample occurs under the electron beams of the SEM.[1b,d] Thereby, in many cases, the obtained resolution of the SEM images is on the micrometer scale and above.

[†] Laboratoire d'Electrochimie Moléculaire et Macromoléculaire, Synthèse et Electrosynthèse Organiques.
[‡] Laboratoire de Chimie du Solide et Inorganique Moléculaire.

10.1021/jp051846y CCC: $30.25
Published on Web 07/16/2005

In this connection, the development of scanning probe microscopy, SPM (and especially atomic force microscopy, AFM), opened up new horizons for in situ morphological studies of electrochemical systems.[7] In recent studies,[8] we have designed a special homemade cell for working in dry organic solvent under an inert atmosphere (argon), which allows the in situ observation of surface electrochemical processes by AFM (EC-AFM).[9] The setup was tested with the cathodic treatment of platinum when the supporting electrolyte was NaI. In situ monitoring of the surface let us observe the growth of the modification directly in the liquid phase.[8] In the present work, we performed more systematic in situ morphological investigations of the cathodic modification of platinum surface, using EC-AFM at the local scale. Our purpose was to answer to several questions related to the electrochemical reversibility of the processes, surface reconstruction, and effects due to the nature of the supporting electrolyte. Different types of supporting electrolytes were investigated by in situ EC-AFM, namely, alkaline iodides (NaI, KI, CsI) and quaternary ammonium iodides in which the chain length of the quaternary ammonium was changed (NMe_4I, NBu_4I, and $NHex_4I$). For the sake of simplification, the electrolyte anion was kept the same in all experiments.

Experimental Section

EC-AFM in Dimethylformamide. The electrochemical "reduction" of platinum was investigated by in situ EC-AFM in dry and deoxygenated DMF. AFM requires the use of a very flat sample for allowing the scanner to follow the surface morphology, and this condition renders difficult the experiments with native samples of platinum. Our samples were prepared by dc sputtering of Pt onto (100)MgO, leading to a distribution of (100)Pt platelets (around 100−200 nm size and an average thickness around 50 nm) (see below for details). By adjustment of the experimental conditions, different general patterns can be obtained where the platinum areas are connected or not.[10] We selected the preparative conditions in order to get connected Pt areas and the same morphology was used in all the experiments. Under such conditions, the sample is macroscopically a conductor and behaves like a single very flat native electrode. Samples prepared by this technique have several advantages: (i) the average roughness of the platelets is low (around 2 nm) and their crystallographic orientations correspond to a fully defined (100)Pt surface; (ii) the sample behaves like a native electrode; (iii) patterns are easily recognizable, which make the observations easier by comparison with an unmodified sample. The morphology of the Pt modifications was characterized by contact-mode atomic force microscopy on a PicoSPM II instrument from Molecular Imaging (Tempe, AZ). In this microscope, the scanner carrying the Si_3N_4 cantilevers (nanoprobes, spring constant 0.12 $N \cdot m^{-1}$) is located beneath the sample (top-down scanning) and can easily be used with our homemade cell.[8] The presented images correspond to typical experiments as stable imaging was obtained in most cases and were recorded with a 10 μm-range scanner. The details of the electrochemical cell and modifications of the AFM setup have been described before.[8] The cell was a three-electrode type setup. The working electrode that is also the AFM sample has a 5×5 mm^2 size and is fixed onto the bottom of the cell by two wires to avoid any movement during the AFM scanning. The reference electrode was an Ag wire covered with $AgNO_3$ quasi reference electrode. Its potential was checked versus the ferrocene/ferrocenium couple (considering $E^\circ = 0.400$ V/SCE) and potentials were scaled versus the SCE electrode. The counterelectrode was made by twisting 50 μm platinum wire and placing it all around the cell. This geometry gets an almost homogeneous modification of the sample. All experiments were performed under inert gas (argon) to limit the introduction of water and oxygen, because the electromodifications of platinum are highly sensitive to the presence of water and oxygen.[1]

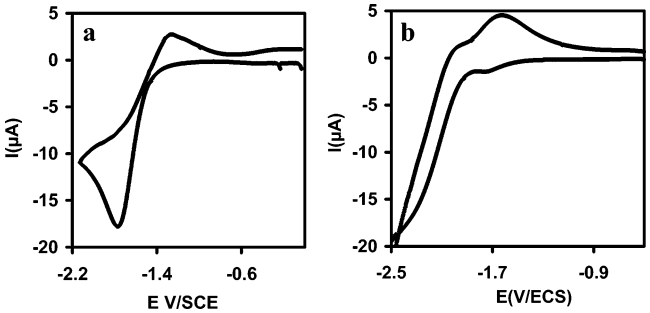

Figure 1. Cyclic voltammetry of 1 mm diameter platinum disk electrode in (a) 0.1 $mol \cdot L^{-1}$ NaI and (b) 0.1 $mol \cdot L^{-1}$ NBu_4I in DMF. Scan rate was 0.1 $V \cdot s^{-1}$.

Surface Preparation. The platinum working electrodes, which were also the AFM substrates, were prepared by dc sputtering of Pt, applying a voltage of −2.3 kV, under an argon pressure of 5×10^{-2} mbar, onto (100)MgO single-crystal substrates (5×5 mm^2) heated at 450 °C.[10] $\theta-2\theta$ X-ray diffraction showed the (100) orientation of the Pt films and the narrow rocking curve recorded on the 200 reflection (full width at half-maximum, fwhm, of 0.33°) showed the high crystalline quality of the film. X-ray diffraction φ-scan of the 220 Pt reflection evidenced the epitaxial growth of the Pt films (Figure 7). From this process, distributions of (100)Pt platelets were obtained with 100−200 nm surfaces and an average thickness around 50 nm. We have previously shown that this type of structured sample allows clean observation and control of the surface electrode by AFM.[8]

EQCM Experiments. Setup and experimental procedures for the electrochemical quartz crystal microbalance were the same as previously described in ref 1.

Chemicals. Alkaline iodide MI (M = Cs, K, Na) and quaternary ammonium iodide AI (A = Bu_4N, Et_4N, Hex_4N) used at 0.1 $mol \cdot L^{-1}$ concentration in solution, from Fluka (electrochemical grade) were used as supporting electrolyte without any further purification. Dry *N*,*N*-dimethylformamide (DMF, puriss) was purchased from Fluka and stored over molecular sieves. All solutions were deoxygenated by bubbling argon for 20 min before each experiment.

Results and Discussion

Cyclic Voltammetry Investigations. Several effects due to the cation changes were evidenced by cyclic voltammetry investigations. Figure 1 displays two typical cyclic voltammetries carried out in a dry DMF solution containing 0.1 $mol \cdot L^{-1}$ NaI (panel a) or 0.1 $mol \cdot L^{-1}$ NBu_4I (panel b) on a solid platinum disk electrode. With NaI, the voltammogram shows a well-defined quasi-reversible redox system in agreement with the typical patterns already reported.[1] The electrochemical reduction peak (peak potential, $E_p = -1.7$ V/SCE at a scan rate of 0.1 $V \cdot s^{-1}$) can be ascribed to the reversible formation of the reduced phase [Pt_2^-, Na^+, NaI] ($n = 2$ in the case of NaI).[1] A nearly reversible electrochemical system was also observed with NBu_4I as supporting electrolyte but the process occurs at more negative potentials ($E_p = -2.4$ V/SCE at 0.1 $V \cdot s^{-1}$).

The same general electrochemical features were found with the other supporting electrolytes on a solid platinum disk

TABLE 1: Reduction Potentials for the Pt Modifications for Different Supporting Electrolytes

supporting electrolyte	peak potential[a] (V/SCE)
NaI	−1.7
CsI	−1.8
KI	−1.9
Me_4NI	−2.1
Bu_4NI	−2.4
Hex_4NI	−2.5

[a] Peak potentials were measured by cyclic voltammetry at 0.1 $V \cdot s^{-1}$.

electrode: a quasi-reversible redox system was observed for which the location of their electrochemical reduction peak depends mainly on the nature and size of the electrolyte cation (see Table 1).

As noticed with Bu_4NI, for the other quaternary ammonium salts the potential required for the platinum modification was found to be more negative as compared with the alkaline iodide salts. It became even more negative when the chain length was increased (i.e., when the electrolyte cation becomes larger), indicating that the insertion of bulkier salts into the platinum and the formation of the iono−metallic phases requires more energy.

The negative values of the potentials in Table 1 suggest that [Pt_n^-, M^+, MX] should exhibit strong reductive properties,[1] which explain that when the sample is exposed under air, the reduced platinum phases are not stable and react with dioxygen. We have previously observed that the initial structure of the sample was recovered after a long-time exposure under air, suggesting that the [Pt_n^-, M^+, MX] could also be electrochemically reoxidized. To test this idea, we prepared two platinum substrate electrodes that were cathodically modified in DMF solution containing 0.1 $mol \cdot L^{-1}$ NaI and examined them by SEM after treatments. One of them was electrochemically reoxidized; that is, we applied a positive potential (more positive than the peak potential corresponding to the anodic process), typically more positive than −0.5 V/SCE during 10 s. Figure 2compares the SEM images of the two platinum surfaces (panel b and c) with that of the initial surface recorded before the cathodic modifications (panel a). In Figure 2a, one can observe large flat areas of platinum with deep holes representing the surface porosity. In Figure 2b, the SEM image shows the appearance of small grains in the platinum platelets after the cathodic treatment. The reoxidized surface (see Figure 2c) exhibits a structure very similar to the initial one, suggesting that the initial morphology of the sample can be recovered (compare Figure 2 panels a and c).

In Situ EC-AFM Investigations: Alkaline Iodides. To monitor the reversibility of the cathodic modification of platinum at the micrometer scale, we must avoid removing the electrode from the solution because of the sensitivity of the samples to dioxygen. With that purpose, we realized in situ EC-AFM imaging of the modified platinum surfaces, on which the electrochemical transformations and the AFM imaging were simultaneously realized. Our main interest was to follow the evolution of the platinum electrode morphology as a function of the injected charge and the nature (organic or inorganic) of the supporting electrolyte and appreciate the reversibility of the whole process. Three alkaline iodides were considered, and for each of them, we first checked by AFM the stability of the Pt sample in the solution (DMF + 0.1 $mol \cdot L^{-1}$ of the salt). The sample was immersed during 1 h and no visible modification of the surface was observed by comparison with the original substrate, confirming that the Pt layers are stable under these experimental conditions. Next, the cathodic modifications were

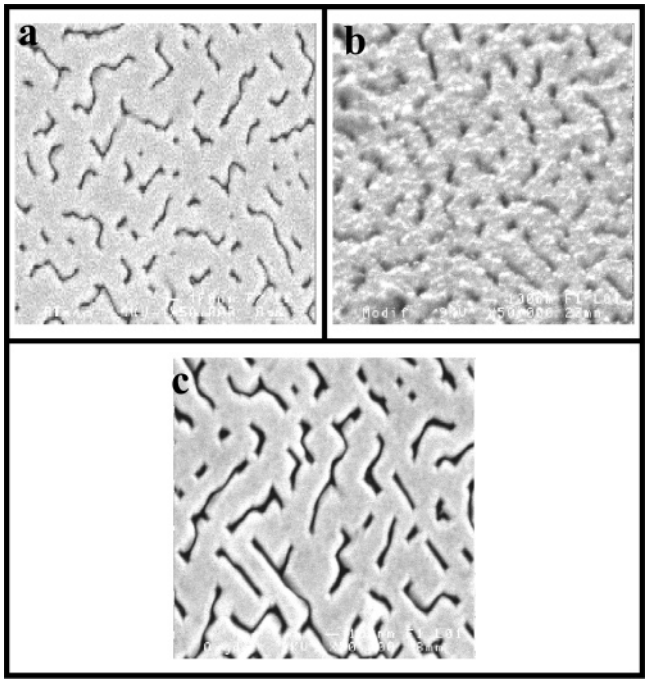

Figure 2. SEM images of platinum deposited on (100)MgO: (a) initial platinum substrate; (b) after electrochemical modification in 0.1 $mol \cdot L^{-1}$ NaI in DMF, reduction with a charge density of 24 $mC \cdot cm^{-2}$; (c) after reduction followed by an electrochemical reoxidation.

completed. The electrochemical procedure was the same for all the experiments. The charge injection was performed by repetitive scans. After each scan, the sample was disconnected but maintained in the DMF solution under argon. The injected charge was quantified and the image was recorded. Between 3 and 5 images were recorded after each electrochemical charge injection to appreciate the stability of surface changes during the observation times. In all cases, we did not observed any significant modification between the different images (the recording time was around 250 s), showing that samples did not evolve for at least 10 min.

Typical AFM topographic images, carried out in solutions containing 0.1 $mol \cdot L^{-1}$ NaI in dry DMF, are gathered in Figure 3. They show the Pt sample before and after different potential scans. The visible bright and dark areas in Figure 3a correspond respectively to the platinum plates separated by 10 nm deep holes due to the epitaxial growth of the Pt films in the chosen deposition conditions. After a cathodic scan limited in potential range with a boundary potential E_r more positive than −0.8 V, the AFM image represented in Figure 3a did not show any significant change. On Figure 3b, we started applying a cathodic polarization with a boundary potential E_r corresponding to the threshold of the voltammetric step ($E_r = -1.4$ V/SCE). Small grains grew immediately on the Pt platelets (see Figure 3b) but the initial structure of the sample constituted of platinum plates and deep holes remained. When the reverse potential became even more negative ($E_r = -1.7$ V/SCE) and the charge passed in the sample increased (e.g., after the injection of a charge density of around 70×10^{-3} $C \cdot cm^{-2}$), tremendous changes in the metal surface appeared (see Figure 3c). The holes and the flat platelets specific to the initial morphology completely disappeared and were replaced by large spheroids with diameters around 150 nm. Consequently, the average roughness increased to reach a value of 70−100 nm. These impressive changes in the morphology concomitantly with a surface swelling obviously reflect the insertion of species into platinum. It is likely that the formation of the iono−metallic platinum phase [Pt_n^-, Na^+,

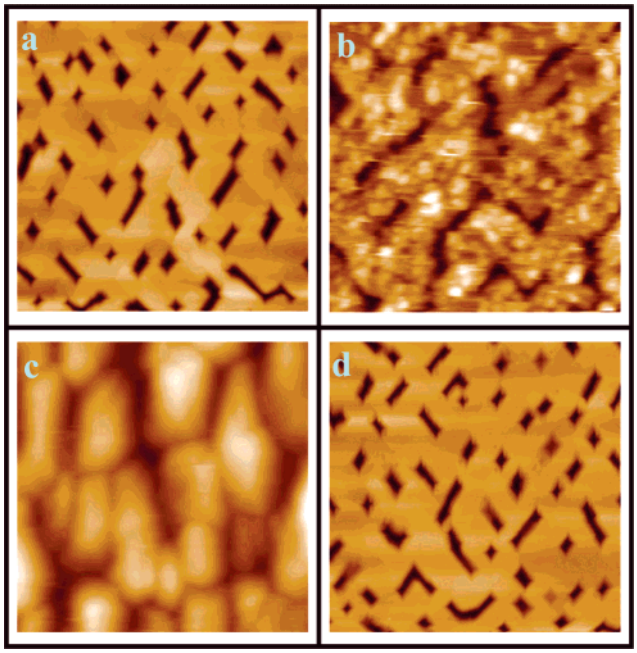

Figure 3. In situ EC-AFM images of the platinum modification in NaI (0.1 mol·L^{-1}) in DMF: (a) in solution before any charge injection; (b) after reduction with a charge density 3.2 mC·cm^{-2}; (c) after reduction with a charge density of 70 mC·cm^{-2}; (d) after electrochemical reoxidation. Image scan size is 3 × 3 μm^2.

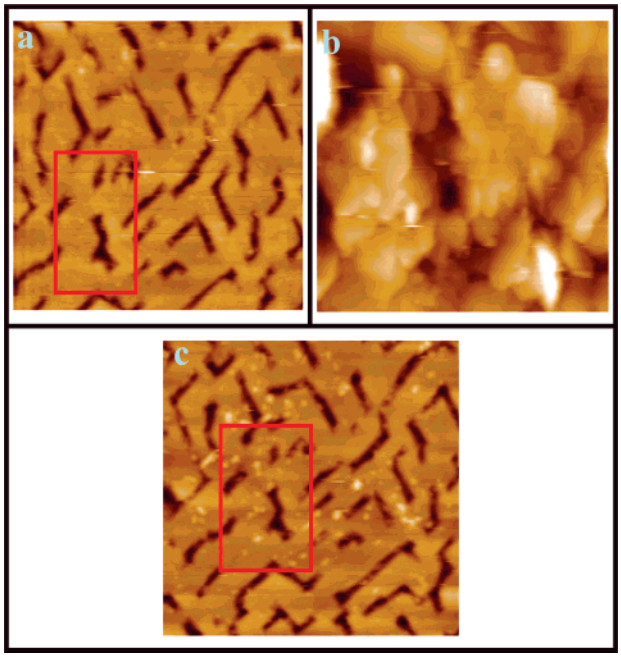

Figure 4. In situ EC-AFM images of the platinum modification in NaI (0.1 mol·L^{-1}) in DMF: (a) in solution before any modification; (b) after reduction with charge density of 120 mC·cm^{-2}; (c) after electrochemical reoxidation. Image scan size is 3 × 3 μm^2.

NaI] is associated with an increase of volume that is attested by the rise of the surface roughness.

The total saturation of the platinum crystal cannot be reached in the course of a voltammetric scan and thus the global value of the stoichiometry, *n*, in the phase structure remains much larger than 2. If we continue with further cathodic modification, that is, injecting higher charge densities, we detected areas without Pt. This observation shows that the entire Pt layer was converted and indicates that the adhesion forces between the new phase and the substrate MgO are too low to maintain the deposit platinum on the MgO substrate, and thus the layer disaggregated into the solution.

Even if crystallographic data are not available for [Pt_2^-, Na^+, NaI], its crystallographic parameters are likely to be different from those of (100)Pt, with the result that the electrogenerated phase is not compatible with the MgO surface. From those observations, we can now conclude that the modification reaction starts at the liquid electrolyte/platinum interface and then proceeds inside platinum until the iono−metallic phase finally reaches the MgO substrate and causes the irreversible layer desegregation and dispersion into the solution.

In a situation where the injected reductive charge remained sufficiently low to avoid the desegregation of the layer, a (0.0 V) potential was applied to the sample to reoxidize the previously produced [Pt_n^-, Na^+, NaI]. Figure 3d shows the morphology of the surface after this reoxidation treatment. The most remarkable feature is that the morphology of the sample is similar to the initial pattern of the virgin sample (compare Figure 3 panels a and d).

This procedure, reduction to produce [Pt_n^-, Na^+, NaI] followed by a total reoxidation process, was performed several times (around 10 times) without any considerable changes or loss of the sample morphology, showing that the cathodic process is fully reversible. This result falls in line with the previous EQCM measurements where quartz crystal microbalance analyses, performed on both native Pt foils and platinum deposit on gold, showed that, after a complete reduction−oxidation cycle, samples had recovered their original mass.[1d] It is noticeable that if we observe total microstructural reversibility, the injected charge required to reoxidize the modified platinum was lower than that needed for carrying out the platinum modification, certainly because of the competitive reduction of the residual water.

The same EC-AFM experiments were performed with two other alkaline iodides, CsI and KI (see Figures 1S and 2S in the Supporting Information). On the whole, observations similar to those reported in Figure 3 were obtained, especially concerning the remarkable reversibility of the process. For all alkaline iodide salts, it was possible to recover the initial structure of the Pt sample modification after electrochemical reoxidation or after exposure the modified sample, for a few hours, under air.

To go further with the possible extension of the reversibility, a final experiment was performed with NaI, in which we injected the maximum charge just before observing the desegregation of the sample (120 mC·cm^{-2}). Considering a homogeneous modification on the entire sample surface, this value of the injected charge corresponds to a superficial modification around 50% of the platinum layer.[11] We managed in this experiment to record the AFM images for the cathodic modification and the reoxidation in the same area of the sample.

Such an experiment was difficult to achieve with sufficient precision, since in several instances, we have to move up the tip after electrochemical modification due to the large variations of the surface topography that cannot be compensated by the AFM scanner and this procedure induces a drift of the tip position. Figure 4 panels a and b show the AFM images of the platinum substrate in solution before and after cathodic modification, respectively. In Figure 4b, large and impressive changes are visible. The holes and flat terraces of the initial morphology have completely disappeared. After electrochemical reoxidation, the AFM image (Figure 4c) shows that, even in these aggressive conditions, the initial structure of platinum is still fully recovered. Moreover, the resulting topography shows identical patterns of platinum since the same deep hole is found as compared with the initial image (Figure 4a; see the red-marked

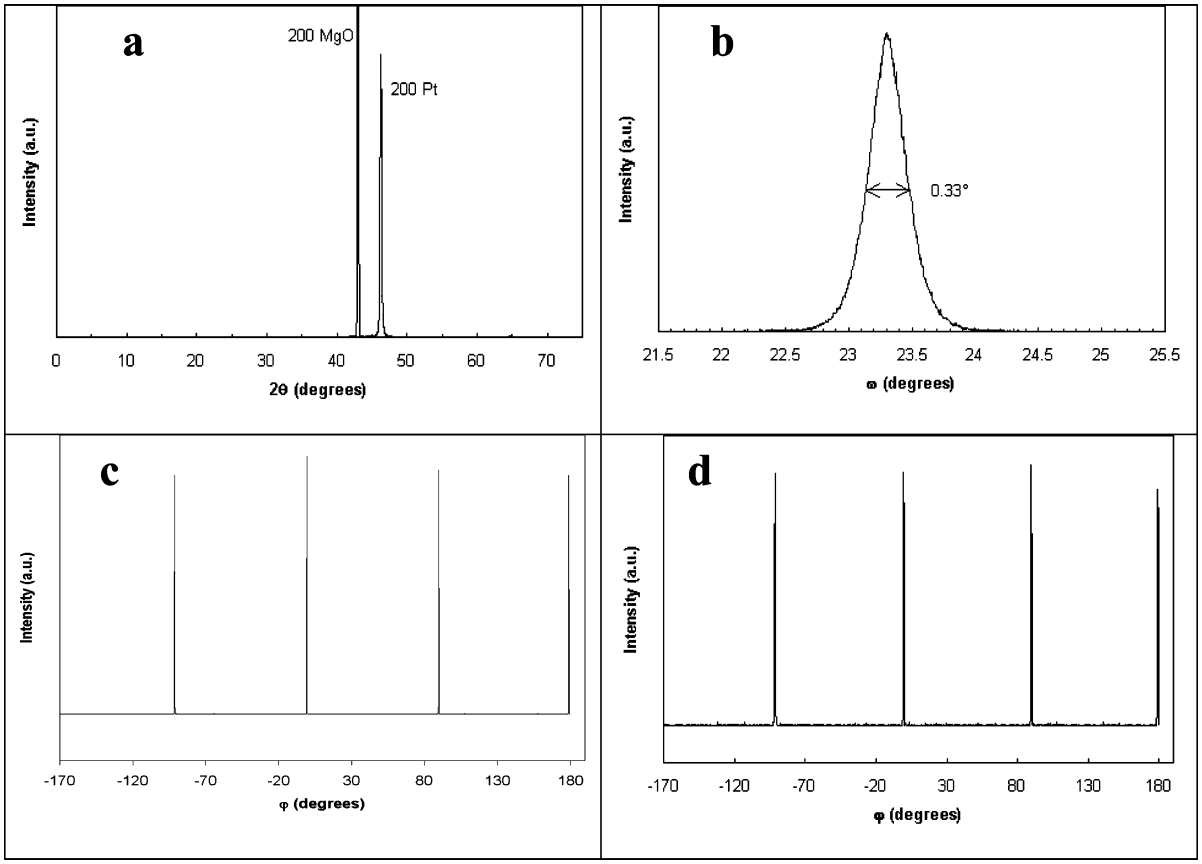

Figure 5. X-ray analyses of the platinum modification in DMF with NaI after a full cycle of reduction and reoxidation of the sample. (a) $\theta-2\theta$ X-ray diffraction pattern evidencing the (100) orientation of the Pt film, after cycle of reduction−oxidation. (b) X-ray diffraction ω-scan performed on the 200 reflection of Pt after cycle of reduction−oxidation (as a standard, the fwhm of the ω-scan performed on the single-crystal substrate was 0.027°). (c, d) X-ray diffraction φ scans recorded for the 220 reflections of (c) MgO and (d) Pt after a cycle of reduction−oxidation.

area). This result reveals the large electrochemical structural reversibility of the modified platinum that can be a great advantage in several applications, for example, in those related to energy storage and localized energy storage when the areas of platinum sample are not connected.

X-ray Diffraction Investigation: NaI. To confirm the reversibility of the platinum modification, X-ray diffraction analyses were performed on Pt films deposited on (100)MgO, after the electrochemical cathodic modifications and after its reoxidation (see Figure 5). After the full reduction−oxidation cycle, all the samples exhibited similar diffraction patterns; that is, no variation was observed, either for the 2θ diffraction angles on the $\theta-2\theta$ diffraction patterns or for the width of the ω-scan and the φ-scan. All the diffraction patterns were the same as for the initial sample.[8a] These results indicate that the Pt lattice parameter was not changed and that the crystalline quality of the epitaxial film was not affected by the full cycle of reduction−oxidation. In particular, no misorientation along the growth direction was detected, as the width of the ω-scan peak was the same. Similarly, the in-plane ordering was not affected by the reduction−oxidation cycle (quality of φ-scan pattern was preserved). These experiments confirm the AFM observations about the full reversibility of the electrochemical process.

In Situ EC-AFM and EQCM Investigations: Tetraalkylammonium Salts. In this series of experiments, we similarly performed the cathodic modification of platinum surfaces in solutions containing a quaternary ammonium salt in dry DMF instead of an alkaline iodide salt. Modification was carried out with the same substrate used above, under the same general experimental conditions and followed by EC-AFM. As reported in Table 1, reduction peak potentials depend on the nature and size of the tetraalkylammonium cation. It is thus interesting to understand how the cation size influences both the structural changes upon cathodic modifications and the reversibility of the whole process, taking into account that the reduction potential becomes more negative when the bulkiness of the cation is increased ($E_{p\,Me_4NI} > E_{p\,Bu_4NI} > E_{p\,Hex_4NI}$). Figure 6shows EC-AFM images of platinum electrode under electrochemical treatment in solutions containing tetramethylammonium. As we observed for the alkaline iodides, the modification of platinum electrode under cathodic polarization starts with the formation of small grains on the platinum terraces (Figures 6b). After larger charge injections, the holes and flat platelets of the initial patterns disappeared and were replaced by spheroids; the average roughness increased to reach values around 120−150 nm (Figure 6c) Concerning the reversibility, we held the modified surface at a potential around 0 V for a few seconds and then reexamined the sample in solution by AFM.

As seen in Figure 6d, the surface recovered its initial structure showing that the cathodic process is also reversible when the supporting electrolyte is a tetraalkylammonium salt. Similar results were obtained with tetrahexylammonium iodide (Figure 3S in the Supporting Information).

This reversibility can be compared by means of coulometric and EQCM experiments. The mass variations reflect the behavior of golden quartz covered with a thin platinum layer during cathodic polarization (gold is not modified by the cathodic treatment). During the potential scan when the inversion potential was not too negative (i.e., for a value located before the mass peaks in Figure 7), the mass changes versus the applied potential were almost reversible.[1] The behavior changes when

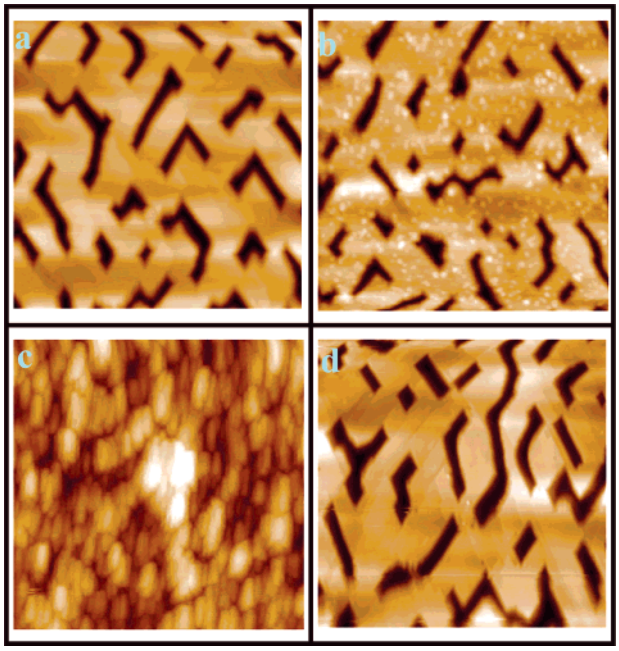

Figure 6. In situ EC-AFM images of the platinum modification in Me_4NI (0.1 mol·L^{-1}) in DMF: (a) in solution before any modification; (b) after reduction with a charge density 0.43 C·cm^{-2}; (c) after reduction with a charge density of 3.86 C·cm^{-2}; (d) after electrochemical reoxidation. Image scan size is 3 × 3 μm^2.

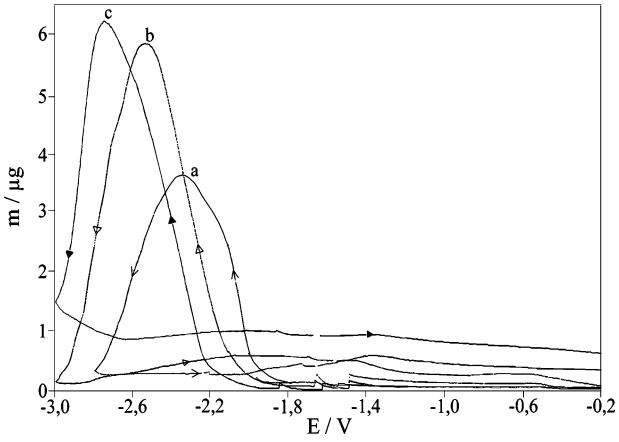

Figure 7. EQCM measurements: mass changes of a golden quartz covered with a thin platinum layer as a function of the applied potential for several tetraalkylammonium salts, (a) tetrabutylammonium, (b) tetrahexylammonium, and (c) tetraoctylammonium. Salt concentration was 0.1 mol·L^{-1}; the solvent was DMF. Scan rate was 10 mV·s^{-1}.

the inversion potential of the scan was set to a more negative value. Figure 7 shows the total mass change as a function of the applied potential for several tetraalkylammonium salts for large potential scans in such case.

For the three investigated tetraalkylammonium salts, the mass of the sample increases when the applied potential approaches the value required for the modification until a maximum mass uptake is reached. We can notice that the potential required for the modification becomes more negative when the chain length of the tetraalkylammonium cation is increased, in agreement with the cyclic voltammetry experiments (see the values of Table 1). After the maximum, a very sudden loss of mass occurred and the final mass at the end of the potential cycle was lower. Other EQCM experiments show that the modification of the platinum did not occur at very negative potential. This phenomenon, which was only observed with the tetraalkylammonium salts and not with the alkaline iodides (Figure 4S in the Supporting Information), corresponds to the dissolution of the platinum phases at more reducing potential. Actually, tetraalkylammonium cations $^+NR_4$ are known to be cathodically cleaved at very negative potential according to the following mechanism:[12]

$$^+NR_4 + e^- \rightarrow R_3N + R\bullet$$

$$R\bullet + e^- \rightarrow R^-$$

$$R^- + H^+ \rightarrow RH$$

The loss of mass shows that the iono−metallic phase is reduced following a similar reaction scheme in the modified platinum:

$$[Pt_n^-, {}^+NR_4, NR_4X] + e^- \rightarrow nPt + R^- + R_3N + R_4NX$$

As a consequence of this observation, we can deduce that the chemical structure of the tetraalkylammonium cation is not modified in the phase $[Pt_n^-, {}^+NR_4, NR_4X]$ and that the negative charge is indeed localized on the platinum atoms. An opposite situation as the localization on $^+NR_4$ should lead to the formation of the corresponding amine.

Another major difference between the modifications performed with the organic and inorganic salts is the quantity of injected charge required to create significant morphological modifications. For example, to obtain a grain size around 100 nm, the values of the injected charge were around 50 × 10^{-3} and 3.5 C·cm^{-2} for alkaline iodide and tetraalkylammonium iodide, respectively.[13] Considering that we should not expect smaller volumes changes when the bulkier $^+NR_4$ cation is used, this difference indicates that the yield to produce the reduced phase is much lower when the salt is a tetraalkylammonium iodide. This can be related to the more negative potential required for tetraalkylammonium salts, which should favor the occurrence of other cathodic processes that are also charge-consuming. When the iono−metallic interface is formed, the morphological reversibility of the modification after reoxidation under air or by electrochemistry is similar for both electrolyte types. However, in the case of the tetraalkylammonium salts, the consumption of the modified platinum is also observed at very negative potentials, for which the electrogenerated phases can also be reduced.

Conclusion

The EC-AFM investigations have confirmed at the submicrometer scale and in situ conditions that when a platinum electrode is maintained under cathodic polarization in a dry organic solvent like DMF containing a supporting electrolyte (alkaline or tetraalkylammonium salts), this leads to the formation of iono−metallic platinum phases $[Pt_n^-, M^+, MX]$. The same general results were obtained with the alkaline and tetraalkylammonium salts. Upon charge injections, the modification begins at the surface of the electrode by the formation of small grains along the platinum terraces. These spherical grains grow when the injected charge increases, until a dramatic change was obtained in the morphology of the sample corresponding to the formation of an iono−metallic layer. The amplitude of the modification essentially depends on the quantity of charge injected into the platinum electrode during the electrochemical treatment. The most remarkable feature of this process is the full reversibility of the structural changes. Upon reoxidation of the modified electrode, the initial structure of the sample is recovered. As evidenced by the EC-AFM images

(and confirmed by X-ray diffraction analyses for alkaline salts), the cycle—cathodic treatment to produce [Pt_n^-, M^+, MX] followed by a reoxidation of the sample to regenerate the platinum metal—can be repeated several, up to 10, times without significant changes of the recovered structure. This perfect return (or almost perfect) of the Pt layer to its initial metallic structure provides to the electrochemical transformation a kind of memory effect that could find applications in area like energy storage or nanotechnology, for example, applications based on the reversible transformation of a conducting Pt microcrystal to an iono−metallic form. It is also noticeable that the formation of reduced metallic phases under electrochemical transformations has been observed with other metals (Ni, Pd, etc.), which may also open new routes in these fields.

Acknowledgment. L. Burel (LCSIM technical staff, Rennes) is warmly acknowledged for her help in Pt film deposition.

Supporting Information Available: EC-AFM experiments on the cathodic modification of Pt deposited on MgO performed with CsI KI and NhexNI as supporting electrolytes and EQCM measurements of mass changes of a golden quartz covered with a thin Pt layer as a function of the applied potential with NaI. This material is available free of charge via the Internet at http://pubs.acs.org.

References and Notes

(1) (a) Cougnon, C.; Simonet, J. *Platinum. Met. Rev.* **2002**, *46*, 94. (b) Cougnon, C.; Simonet, J. *Electrochem. Commun.* **2002**, *4*, 266. (c) Cougnon, C.; Simonet, J. *Electroanal. Chem.* **2002**, *531*, 179. (d) Simonet, J. *Electrochem. Commun*. **2003**, *5*, 439.

(2) (a) Zintl, E.; Woltersdaf, G. Z. *Electrochem.* **1935**, *41*, 876. (b) Zintl, E.; Dullenkopf, G. Z. *Phys. Chem. B* **1932**, *16*, 183.

(3) (a) Tomashova, N. N.; Kiseleva, I. G.; Astakhov, I. I.; Kabanov, B. N. *Elektrokhimiya* **1968**, *4*, 471. (b) Teplitskaya, G. L.; Astakhov, I. I. *Elektrokhimiya* **1970**, *6*, 379. (c) Teplitskaya, G. L.; Astakhov, I. I. *Elektrokhimiya* **1972**, *8*, 1199. (d) Baranski, A. S.; Fawcett, W. R. *J. Electrochem. Soc*. **1982**, *129*, 901. (e) Kariv-Miller, E.; Svetlicic, V. *J. Electroanal. Chem*. **1985**, *205*, 319. (f) Kariv-Miller, E.; Andruzzi, R. *J. Electroanal. Chem*. **1985**, *187*, 175. (g) Svetlicic, V.; Kariv-Miller, E. *J. Electroanal. Chem.* **1986**, *209*, 91. (h) Ryan, C. M.; Svetlicic, V.; Kariv-Miller, E. *J. Electroanal. Chem.* **1987**, *219*, 247. (i) Gewirth, A. A.; Niece, B. K. *Chem. Rev.* **1997**, *97*, 1129.

(4) Bard, A. J.; Faulkner, L. R. *Electrochemical Methods: fundamentals and applications*, 2nd ed.; John Wiley & Sons Inc.: New York, 2000.

(5) Simonet, J.; Labaume, E.; Rault-Berthelot, J. *Electrochem. Commun.* **1999**, *1*, 252.

(6) Cougnon, C.; Simonet, J. *Electrochem. Commun.* **2001**, *3*, 209.

(7) (a) AFM imaging can be operated under ambient conditions and in a liquid environment, which opens up exciting possibilities to follow electrochemical process that occur onto the electrode surfaces. For some general references about EC-AFM see for example (b) Kariuki, J. K.; McDermott, M. T. *Langmuir* **1999**, *15*, 6534. (c) Liu, S.; Tang, Z.; Wang, E.; Dong. S. *Langmuir* **1999**, *15*, 7268. (d) Brooksky, P. A.; Downard, A. J. *Langmuir* **2004**, *20*, 5038.

(8) (a) Bergamini, J.-F.; Ghilane, J.; Guilloux-Viry, M.; Hapiot, P. *Electrochem. Commun.* **2004**, *6*, 188. (b) Cougnon, C.; Simonet, J. *J. Electroanal. Chem.* **2001**, *507*, 226.

(9) It is important to note that a solvent like DMF can seriously damage the electronics of an AFM microscope.

(10) (a) Duclère, J. R.; Guilloux-Viry, M.; Perrin, A.; Cattan, E.; Soyer, C.; Rèmiens, D. *Appl. Phys. Lett.* **2002**, *81*, 2067. (b) Duclère J. R. Thèse de Doctorat, Université de Rennes 1, Rennes, France, October 15, 2002.

(11) Considering that one electron is required for two platinum atoms in [Pt_2^-, Na^+, NaI] and an average thickness of 50 nm for the platinum layer.

(12) Dahm, C. E.; Peters, D. G. *J. Electroanal. Chem.* **1996**, *402*, 91 and references therein.

(13) The applied potential was sufficiently positive to avoid the reduction of the phase.